

Dalton Transactions

Accepted Manuscript



This is an *Accepted Manuscript*, which has been through the Royal Society of Chemistry peer review process and has been accepted for publication.

Accepted Manuscripts are published online shortly after acceptance, before technical editing, formatting and proof reading. Using this free service, authors can make their results available to the community, in citable form, before we publish the edited article. We will replace this *Accepted Manuscript* with the edited and formatted *Advance Article* as soon as it is available.

You can find more information about *Accepted Manuscripts* in the [Information for Authors](#).

Please note that technical editing may introduce minor changes to the text and/or graphics, which may alter content. The journal's standard [Terms & Conditions](#) and the [Ethical guidelines](#) still apply. In no event shall the Royal Society of Chemistry be held responsible for any errors or omissions in this *Accepted Manuscript* or any consequences arising from the use of any information it contains.

Layered rare earth hydroxides (LREHs): Synthesis and structure characterization towards multifunctionality

Jianbo Liang, Renzhi Ma, Takayoshi Sasaki*

International Center for Materials Nanoarchitectonics, National Institute for Materials Science, 1-1 Namiki, Tsukuba, Ibaraki 305-0044, Japan

Abstract

Layered rare earth hydroxides (LREHs) represent a new family of layered host compounds that integrate attractive physicochemical properties of rare earth elements with the wide tunability of guest anions. The compounds have attracted significant research attention and potential applications have been found in various fields such as optics, catalysis, bio-medicine and so on. In this perspective, we describe our recent progress in synthesis, structure characterization, and development of functionalities of the LREH compounds. A unique homogeneous alkalization method, in which RE ions are precipitated from a solution containing RE salt, concentrated target anions and hexamethylenetetramine, has been employed to effectively produce highly crystallized LREH samples. A range of anionic forms including chloride-, nitrate-, sulfate- and organodisulfonate-series, have been synthesized and structurally characterized. Two types of cationic rare earth hydroxide layers, $\{[\text{RE}_2(\text{OH})_5(\text{H}_2\text{O})_2]^+\}_\infty$ for the chloride- and nitrate-series, and $\{[\text{RE}(\text{OH})_2(\text{H}_2\text{O})]^+\}_\infty$ for the sulfate- and organodisulfonate-series, are classified. Unique dehydration/rehydration behaviors or thermal phase evolution of the LREH compounds have been revealed and discussed in relation to the intrinsic crystal structures. An outlook for potential applications of LREH compounds as novel anion exchangers, precursors to unique functional oxides, and optical phosphors is described.

1. Introduction

Materials based on rare earth (RE) elements provide valuable functionalities that play key roles in modern industry.¹⁻⁵ Design and synthesis of new compounds with RE elements have become a hot research target, and incorporating them into a special host lattice has attracted enormous interest for seeking new and tailored optical, electrical, and magnetic properties.⁶⁻¹⁰ Among these studies, there has long been desire to incorporate trivalent RE ions to layered double hydroxides (LDHs, chemical formula: $[M^{2+}_{1-x}M^{3+}_x(OH)_2]^{x+}(A^{m-})_{x/m}\cdot yH_2O$; M^{2+} : Mg^{2+} , Co^{2+} , Zn^{2+} ..., M^{3+} : Al^{3+} , Fe^{3+} , Co^{3+} , Cr^{3+} ..., A^{m-} : CO_3^{2-} , SO_4^{2-} , Cl^- , NO_3^- ...; $0.2 \leq x \leq 0.33$.), the well-known layered compounds characterized by facile anion-exchangeability that affords a range of applications in fields of catalysis, environments, energy, biology, and so on.¹¹ However, because of the large difference in ion radii, isomorphous substitution of trivalent ions in the LDH hosts by RE ions is very difficult. Even in the case that successful incorporation was reported, only limited doping of RE elements was attained.¹²⁻¹⁵ Furthermore, obtained samples were mostly poorly crystalline, which makes it difficult to fully verify the intrinsic doping.¹²⁻¹⁷ In view of these drawbacks, efforts to new multifunctional materials coupling both novel properties of RE elements and anion-exchangeability have not witnessed significant progress.

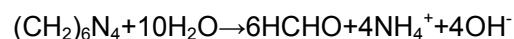
Consequently much attention has turned to the development of a new class of layered compounds built up from pure rare earth hydroxide layers and counter anions, namely, layered rare earth hydroxides (LREHs).¹⁸⁻⁴³ Actually, reports on the synthesis of several rare earth hydroxysalts (we now know that these compounds adopt a layered structure and belong to the LREH family) can be dated back to the late 1960s.¹⁸⁻²² However, at that time, without knowledge of the crystal structure, little attention was paid to exploration of their physicochemical properties, particularly the interplay between the RE element and anions. It is only five or six years ago that the crystal structures were successfully revealed from highly crystallized samples.^{23,25,33,34,38,39} In 2006, the Monge's group first reported the synthesis of new compounds built by cationic rare-earth hydroxides layers, $[R_4(OH)_{10}(H_2O)_4]A$ (R = rare-earth ions, A = intercalated organic anions, 2,6-naphthalenedisulfonate (NDS^{2-}) and 2,6-anthraquinonedisulfonate

(AQDS²⁻)).²³ Later on, LREH compounds intercalated with halide ions were reported from our group and the Fogg's group in the year of 2008.^{25,33} Accompanied by these studies, many novel functionalities associated with facile anion-exchangeability, green catalytic activity and tunable photoluminescence were disclosed. Now, LREH compounds have turned into a new family of multifunctional layered solids that can combine intriguing properties of RE elements and flexible varieties of anionic guests.^{23,24,26-32,35-43}

We have conducted extensive studies on the synthesis of highly crystallized LDH compounds and their exfoliation into unillamellar nanosheets during the past decade.⁴⁴⁻⁴⁸ Based on this experience, we successfully applied a homogeneous alkalization route to produce highly crystallized LREH samples in a range of anionic forms.³³⁻⁴³ The crystal structures of several LREH compounds were analyzed from powder diffraction data and, on the basis of the structural information, their unique dehydration/rehydration behaviors, facile anion-exchangeability, thermal phase evolution and other properties have been well understood. The knowledge about these chemical properties is very useful in the exploration of LREH compounds as multifunctional materials. This perspective provides an overview of our efforts in the development of LREHs as an intriguing class of multifunctional materials.

2. Homogeneous alkalization synthetic strategy

We achieved the synthesis of highly crystallized LDH and brucite-type metal hydroxides by a homogeneous alkalization route.⁴⁴⁻⁴⁸ This method was applied for the synthesis of LREH compounds and found to be very effective in yielding high-quality polycrystalline samples. Typically, an aqueous solution, prepared by dissolving a suitable RE salt, hexamethylenetetramine (HMT, (CH₂)₆N₄), and a source of target anions, was refluxed under N₂ atmosphere in oil bath. Upon heating, HMT undergoes hydrolysis, slowly releasing OH⁻ ions as below:



RE ions are precipitated along with the OH⁻ and target anions to form the crystalline LREH compounds. Under optimized conditions, highly crystallized LREH samples

composed of well developed platy microcrystals could be produced, as shown by the transmission electron microscope (TEM) or scanning electron microscope (SEM) images (Figure 1). X-ray diffraction (XRD) patterns in Figure 2 show a series of intense basal reflections as well as sharp non-basal peaks, suitable for the structure determination. This method enables the preparation of various anionic forms of LREH compounds, for example, the chloride-, nitrate-, sulfate-, and organodisulfonate-forms. The RE members can be varied among the lanthanide series according to the guest anionic form. Particularly, solid solutions containing several RE elements can also be conveniently prepared using this method.

Table 1 A summary of the LREH compounds reported in recent studies.

Anions	RE elements	Chemical formula	Phase	Basal spacing / nm	Reference
2,6-naphthalenedisulfonate (NDS ²⁻)	Y	Y ₄ (OH) ₁₀ (NDS) ₄ ·4H ₂ O	Orthorhombic	1.526	23
2,6-anthraquinonedisulfonate (AQDS ²⁻)	Ho,Dy,Yb	RE ₄ (OH) ₁₀ (ANDS) ₄ ·4H ₂ O	Orthorhombic	1.783 for Yb	23
NO ₃ ⁻	Y, Gd-Lu	RE ₂ (OH) ₅ (NO ₃) _x ·xH ₂ O	Monoclinic	0.83-0.92	24
Cl ⁻	Y,Dy,Yb,Er	RE ₂ (OH) ₅ Cl · 1.5H ₂ O	Orthorhombic	Y: 0.837; Dy: 0.841; Er: 0.839; Yb: 0.842, 0.800	25
Br ⁻	Y, Yb	RE ₂ (OH) ₅ Br · 1.5H ₂ O	Monoclinic	Y: 0.835; Yb: 0.835, 0.877	25
Cl ⁻	Nd, Sm-Tm	RE ₈ (OH) ₂₀ Cl ₄ · nH ₂ O	Orthorhombic	0.830-0.870	33,34
NO ₃ ⁻	Sm-Tm	RE ₂ (OH) ₅ (NO ₃) _x ·xH ₂ O	Monoclinic	0.83-0.92	38
SO ₄ ²⁻	Pr, Nd, Sm-Tb	RE ₂ (OH) ₄ SO ₄ · 2H ₂ O	Monoclinic	~0.83	37
[O ₃ S(CH ₂) _n SO ₃] ²⁻	La~Nd, Sm	RE ₂ (OH) ₄ [O ₃ S(CH ₂) _n SO ₃] ₂ ·2H ₂ O	Monoclinic	~1.31 for n=3 ~1.40 for n=4	39

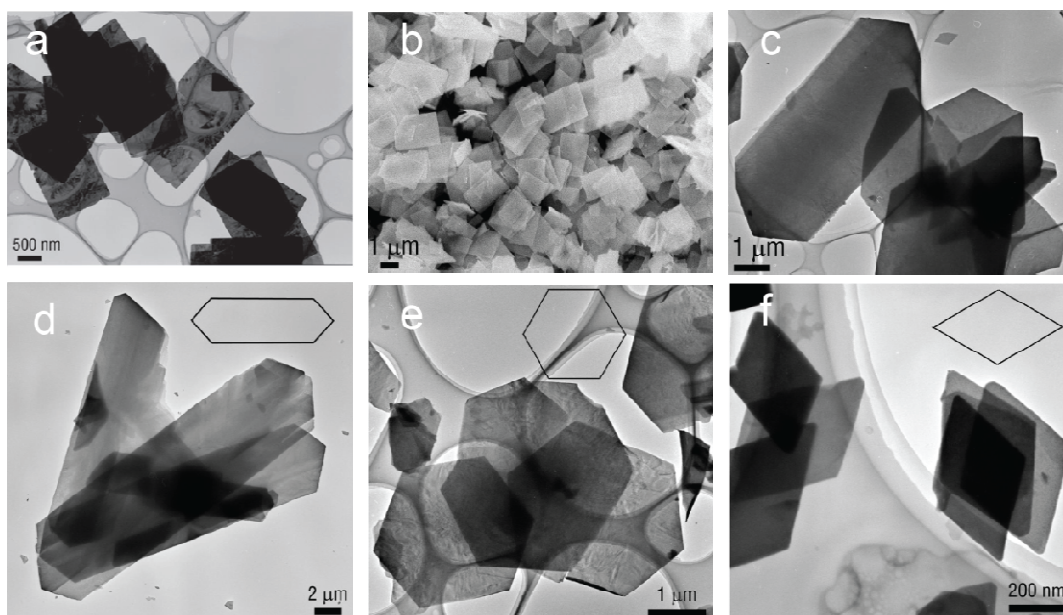


Fig.1 TEM or SEM images of (a) $\text{Eu}(\text{OH})_{2.5}\text{Cl}_{0.5} \cdot n\text{H}_2\text{O}$; (b) $\text{Sm}(\text{OH})_{2.5}\text{Cl}_{0.5} \cdot n\text{H}_2\text{O}$; (c) $\text{Y}(\text{OH})_{2.5}\text{Cl}_{0.5} \cdot n\text{H}_2\text{O}$; (d) $\text{Gd}(\text{OH})_{2.5}(\text{NO}_3)_{0.5} \cdot n\text{H}_2\text{O}$; (e) $\text{Dy}(\text{OH})_{2.5}(\text{NO}_3)_{0.5} \cdot n\text{H}_2\text{O}$; (f) $\text{Er}(\text{OH})_{2.5}(\text{NO}_3)_{0.5} \cdot n\text{H}_2\text{O}$. Adapted with permission from ref. 33 (copyright 2008 Wiley-VCH Verlag GmbH & Co. KGaA) and ref. 34, 35 (copyright 2008 and 2009 American Chemical Society).

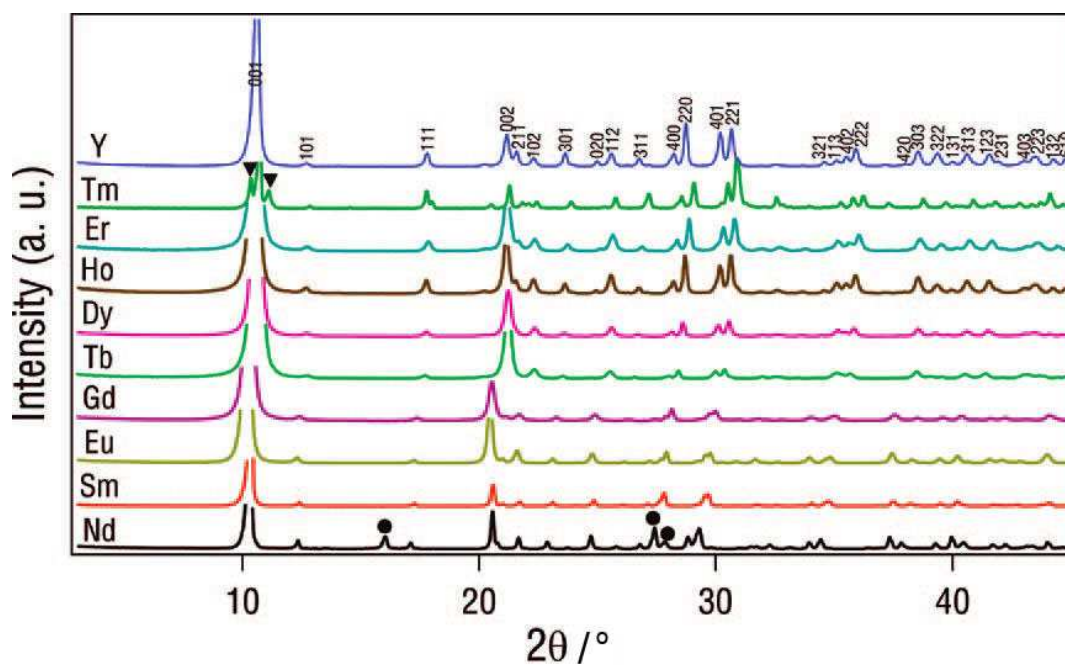


Fig.2 Indexed XRD patterns of $\text{Ln}(\text{OH})_{2.5}\text{Cl}_{0.5} \cdot n\text{H}_2\text{O}$ (Ln: Nd-Tm, Y). The indices are

indicated for the Y member as an example. A trace amount of impurities was detected in the members of Nd and Tm. Adapted with permission from ref. 34. Copyright 2008 American Chemical Society.

3. Characterizations of LREH compounds

3.1 Chloride-series: $\text{RE}(\text{OH})_{2.5}\text{Cl}_{0.5}\cdot n\text{H}_2\text{O}$ (RE: Y, Nd-Tm; $n\sim 0.8$)

LREH compounds with a chemical formula of $\text{RE}(\text{OH})_{2.5}\text{Cl}_{0.5}\cdot n\text{H}_2\text{O}$ were synthesized through the homogeneous alkalization route using NaCl as an anion source. Single-phase samples were obtained in RE members from Sm to Er, while a minor phase of $\text{Nd}(\text{OH})_3$ (~8.1%) coexisted in the Nd sample. Commonly, high relative humidity controlled above 70% was required to maintain the crystallinity.³³ We collected high-resolution synchrotron XRD data, from which their crystal structure was analyzed. A typical example for $\text{Eu}(\text{OH})_{2.5}\text{Cl}_{0.5}\cdot 0.8\text{H}_2\text{O}$ is depicted in Figure 3.

The compound is crystallized in orthorhombic structure (space group $P2_12_12_1$, cell parameters: $a = 1.29152(3)$ nm, $b = 0.73761(1)$ nm, and $c = 0.87016(3)$ nm).³³ In the structure, Eu ions are accommodated in two kinds of sites: one (Eu1) occupies 4c sites, surrounded by seven hydroxyls and one fully occupied H_2O molecule. The other occupies on 2a (Eu2) or 2c (Eu3) sites, bonded to eight hydroxyls and one partially occupied H_2O molecule. Every hydroxyl group is bonded to three Eu ions. Eu ions of the same type are arranged into a row along the b axis, and the rows are alternatively packed along the a axis, forming infinite layers of $\{[\text{Eu}_2(\text{OH})_5(\text{H}_2\text{O})_2]^+\}_\infty$. The chloride ions are accommodated in a well-defined site between two neighboring layers. This aspect is distinct from LDHs where anions are heavily disordered in the interlayer gallery.

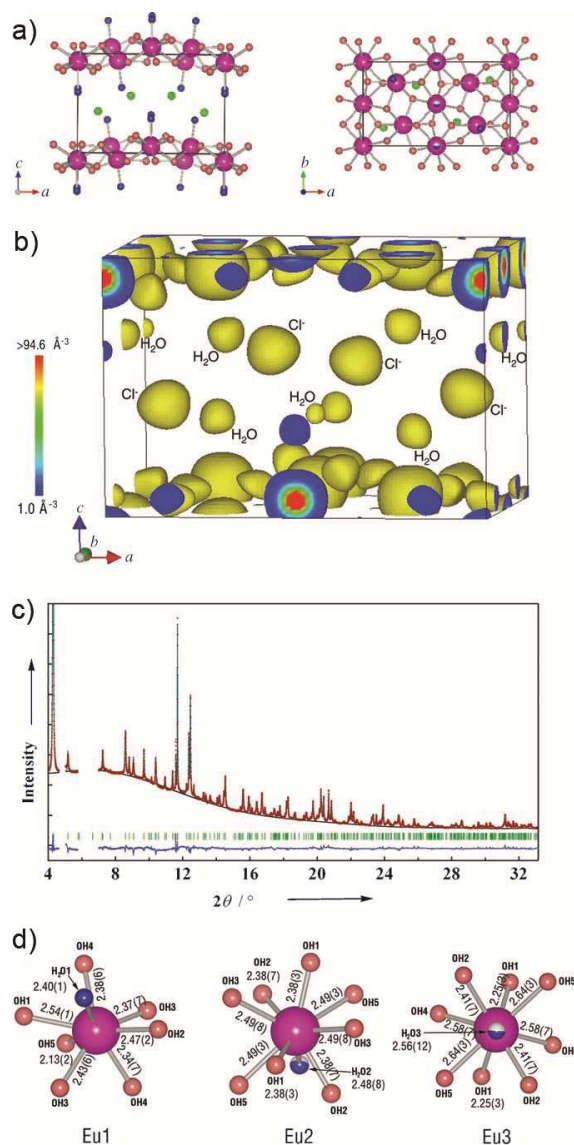


Fig.3 (a) Crystal structure of $\text{Eu}(\text{OH})_{2.5}\text{Cl}_{0.5} \cdot 0.8\text{H}_2\text{O}$; (b) 3D electron-density distribution of the structure; (c) Rietveld refinement profiles; (d) Coordination of the Eu ions in the cationic host layers. Adapted with permission from ref.33. Copyright 2008 Wiley-VCH Verlag GmbH & Co. KGaA.

The series show the progressive decrease in the in-plane cell parameters along the periodic table, which is attributable to the so-called lanthanide contraction.³⁴ Two sets of distinct interlayer distance, ~ 0.870 nm for Nd to Gd, and 0.845 nm for Tb to Er were observed, being associated with different degrees of hydration. The hydration is directly

related to the occupancy of H₂O on the nine-fold coordinated RE ions. Under an ideal condition where all the H₂O sites are fully occupied, the hydration number per unit cell is 8 (4 from eight-fold coordinated REs and 4 from the nine-fold ones). Rietveld analysis results indicate that the hydration number tends to gradually decrease across the series; 7.4, 6.3, and 7.2 for higher hydrated Nd, Sm, and Eu samples, and 5.8, 5.6, 5.4, and 4.9 for lower hydrated Tb, Dy, Ho, and Er samples, respectively. For the Er phase, the occupancy of H₂O on the nine-fold coordinated Er is as low as 0.2, which may be understood in terms of the crowded coordination sphere for this ion. Namely, Er is the smallest ion that represents the limit for adoption of this structure. In this regard, the water molecules are supposed to play a key role in stabilizing the structure of the $\{[RE_2(OH)_5(H_2O)_2]^+\}_\infty$ layers.

The compounds underwent interesting dehydration/rehydration behavior at room temperature, as indicated by in-situ basal spacing measurements at controlled relative humidity (RH).³⁴ For the Nd member, the basal spacing remained virtually constant as a function of RH. For the members of Sm, Eu and Gd, two sets of basal spacing (0.85-0.86 nm, or 0.83-0.84 nm) were observed, indicating two immiscible phases with a different degree of hydration. Abrupt and reversible transformation between these two phases took place in the dehydration and rehydration processes. For the other members, Tb to Tm, and Y, the basal spacing was constant at 0.83 nm throughout the RH range.

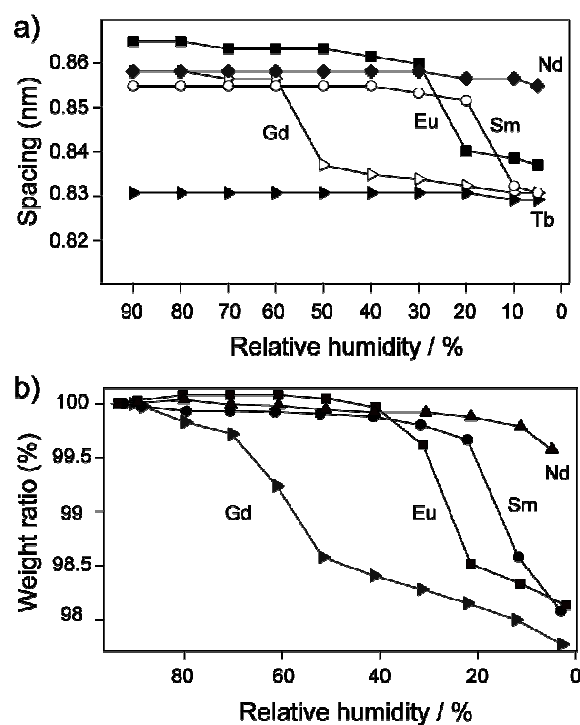


Fig.4 Changes in basal spacing (a) and sample weight (b) of RE(OH)_{2.5}Cl_{0.5}·nH₂O as a function of RH. Adapted with permission from ref.34. Copyright 2008 American Chemical Society.

3.2 Nitrate-series: RE(OH)_{2.5}(NO₃)_{0.5}·nH₂O (RE: Y, Sm-Tm)

Similar to the chloride-series, the nitrate-series of LREH compounds were synthesized by applying concentrated NaNO₃ in the homogeneous alkalization method.³⁵ The samples have a general chemical formula of RE(OH)_{2.5}(NO₃)_{0.5}·nH₂O (RE: Y, Sm-Tm), which are crystallized in monoclinic phase. The in-plane cell parameters *a* and *b* are very close to those of corresponding chloride-members, suggesting a similar layered architecture. On the other hand, the parameter *c* is double the basal spacing, suggesting a complex lattice, involving possible gliding of adjacent layers with respect to each other. Close examination of the indices indicates a systematic absence of *l* = 2*n* + 1 for *h0l*. The possible space group is among *Pc*, *P2/c* and *P2₁/c*. Due to a large number of diffraction peaks overlapping each other, crystal structure determination was hindered even from high-resolution synchrotron XRD data from powder samples.

The dehydration/ rehydration behaviors of the nitrate-series are very different from

those of the chloride-series.³⁵ Figure 5 shows changes in basal spacing against RH in the dehydration and rehydration processes. On the basis of the behaviors, the nitrate-series can be divided into three groups. The group (I) is the Sm sample, the largest RE member in this series. The Sm phase displayed two set of basal spacings: 0.88 and 0.83 nm for high hydration (HH) and low hydration (LH) phase, respectively. The HH phase transformed into the LH phase at about 30% RH, and was not recovered in the reverse process upon humidification. The group (II) contains samples from Eu to Ho, which underwent reversible dehydration-rehydration. In the dehydration process, the basal spacing shrinkage was 0.05 – 0.07 nm, much larger than that of about 0.02 nm observed in the chloride-series samples. The group (III) contains the heavy RE members of Er and Tm, which showed a high hydration state in a wide RH range from 90% to even 5%. The high layer charge density as a consequence of shrinkage in in-plane lattice dimensions for the heavy RE-element phases may favor the adoption of high hydration phase.

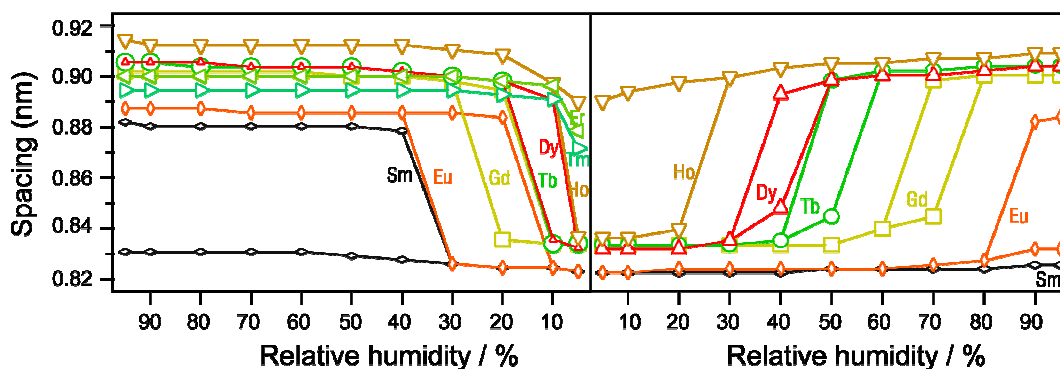


Fig.5 Changes in basal spacing of the nitrate-series LREH compounds as a function of RH. Left: dehydration. Right: hydration. Adapted with permission from ref. 35. Copyright 2009 American Chemical Society.

3.3 Sulfate-series: $\text{RE}_2(\text{OH})_2\text{SO}_4 \cdot 2.0\text{H}_2\text{O}$ (RE: Pr, Nd, Sm ~ Tb)

LREH compounds having a general chemical formula of $\text{RE}_2(\text{OH})_4\text{SO}_4 \cdot 2\text{H}_2\text{O}$ (Ln = Pr, Nd, Sm ~ Tb) were synthesized by refluxing a solution containing $\text{RE}_2(\text{SO}_4)_3$, HMT and Na_2SO_4 .³⁷ These compounds were found to have a monoclinic structure with unit-cell parameters $a \sim 0.63$ nm, $b \sim 0.37$ nm, $c \sim 0.84$ nm, and $90.07 < \beta < 90.39^\circ$. Note the β is approximately equal to 90° . The unit cell, which adopts a base-centered space group, A

$2/m$ (No.12), is subtly distorted from an orthorhombic structure.³⁸

Rietveld analysis reveals that the samples adopt a rigid pillared structure.³⁸ One RE ion is surrounded by nine oxygen atoms, six from OH groups, two from H₂O molecules, and one from SO₄²⁻ ions. Each RE ion is connected with six surrounding neighbors by sharing the μ -₃ OH groups and μ -₂ H₂O molecules, forming an infinite layer of $\{[\text{RE}(\text{OH})_2\text{H}_2\text{O}]^+\}_\infty$ parallel to the *ab* plane. Viewed along the *c* axis, RE ions arrange themselves into a quasi-hexagonal network. SO₄²⁻ ions are covalently bonded to RE ions in a *trans*-bidentate configuration, bridging the $\{[\text{RE}(\text{OH})_2\text{H}_2\text{O}]^+\}_\infty$ layers to form a rigid 3D pillared structure. SO₄²⁻ ions are distorted from the ideal tetrahedral geometry due to the covalent bonding. In the unit cell, SO₄²⁻ ion takes two kinds of orientation, as shown in Figure 6b, resulting in a structural ordering (supported by electron diffraction data). Such an alternate alignment of SO₄²⁻ ions produces void space between them, although not accessible due to the very narrow openings to it.

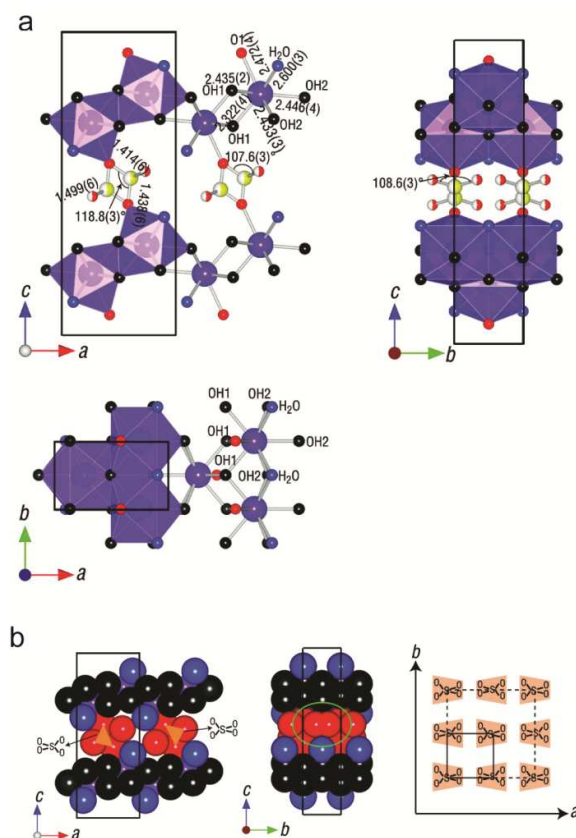


Fig.6 a) Crystal structure of Tb₂(OH)₄SO₄·2.0H₂O, a representative illustration for the

sulfate-series of LREH compounds; b) Space-filling illustration of $\text{Tb}_2(\text{OH})_4\text{SO}_4 \cdot 2.0\text{H}_2\text{O}$. The two kinds of orientation of SO_4^{2-} ions and the voids left between neighboring SO_4^{2-} ions are illustrated. Adapted with permission from ref. 38. Copyright 2011 American Chemical Society.

The strong covalent interaction between RE and SO_4^{2-} ions is confirmed by Fourier transform infrared (FT-IR) spectra (Figure 7).³⁷ In the Tb sample, all the four fundamental modes (ν_1 , ν_2 , ν_3 and ν_4) for SO_4^{2-} ions were observed. The appearance of ν_1 and ν_2 modes, IR inactive for free SO_4^{2-} ions with T_d , proves the lowering of symmetry to C_{2v} . On the other hand, this compound showed three ν_3 modes, which differs to the broad single peak from $\text{Tb}_2(\text{OH})_5(\text{SO}_4)_{0.5} \cdot n\text{H}_2\text{O}$ prepared via anion-exchange process, strongly supporting the chelation of SO_4^{2-} ions to RE ions in a *trans*-bidentate configuration. Furthermore, FT-IR spectra showed that the triple ν_3 modes could be preserved even after the compound was heated to 1000 °C. In the resulting oxide form of $\text{Tb}_2\text{O}_2\text{SO}_4$, SO_4^{2-} ions are bidentately coordinated to Tb^{3+} in a *trans*-configuration,^{49,50} which eventually confirms the covalent bonding nature in the sulfate-LREH compounds.

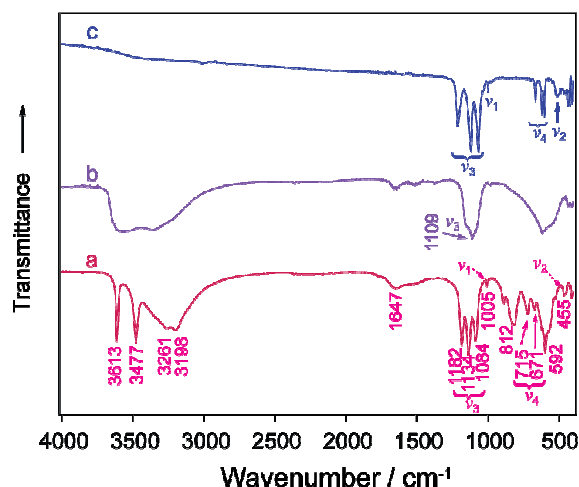


Fig.7 FT-IR spectra of (a) $\text{Tb}_2(\text{OH})_4\text{SO}_4 \cdot 2.0\text{H}_2\text{O}$, (b) $\text{Tb}_2(\text{OH})_5(\text{SO}_4)_{0.5} \cdot n\text{H}_2\text{O}$ prepared by anion-exchange, and (c) $\text{Tb}_2\text{O}_2\text{SO}_4$ by heating sample $\text{Tb}_2(\text{OH})_4\text{SO}_4 \cdot 2.0\text{H}_2\text{O}$ to 1000 °C.

These data confirm that SO_4^{2-} ions are covalently bonded to Tb^{3+} ions in a *trans*-bidentate configuration. Adapted with permission from ref. 37. Copyright 2010

American Chemical Society.

3.4 Organodisulfonate-series: $\text{Ln}_2(\text{OH})_4[\text{O}_3\text{S}(\text{CH}_2)_n\text{SO}_3]\cdot 2.0\text{H}_2\text{O}$ (Ln: La, Ce, Pr, Nd, Sm, $n = 3, 4$)

We simply substituted sodium sulfate with linear organodisulfonate salts, $\text{Na}_2[\text{O}_3\text{S}(\text{CH}_2)_n\text{SO}_3]$, and applied the homogeneous alkalization process, yielding a new series of LREH samples having general formula of $\text{Ln}_2(\text{OH})_4[\text{O}_3\text{S}(\text{CH}_2)_n\text{SO}_3]\cdot 2\text{H}_2\text{O}$ (Ln: La, Ce, Pr, Nd, Sm, $n = 3, 4$).³⁹ These samples are crystallized in monoclinic system with a space group of $P 2_1/n$ (No. 14). The in-plane unit dimensions are almost identical to those of the sulfate-series. On the other hand, the basal spacing is largely expanded from 0.84 nm for the sulfate form to ~ 1.31 nm ($n = 3$) and ~ 1.40 nm ($n = 4$), reflecting the successful incorporation of organic moieties.

The crystal structure, solved from laboratory powder XRD data, is shown in Figure 8 for a representative sample of $\text{La}_2(\text{OH})_4[\text{O}_3\text{S}(\text{CH}_2)_3\text{SO}_3]\cdot 2.2\text{H}_2\text{O}$. This compound can be described as a hybrid framework consisting of cationic host layers of $\{[\text{La}(\text{OH})_2(\text{H}_2\text{O})]^+\}_\infty$ bridged by α,ω -alkanedisulfonate pillars.³⁹ The $\{[\text{La}(\text{OH})_2(\text{H}_2\text{O})]^+\}_\infty$ layer is almost identical to that in the sulfate-series. La ions are coordinated by nine oxygen atoms, among which six are from OH groups, two from H_2O molecules and the last from a SO_3 group of the organic pillar. The La-O(SO_3) bonding distance is calculated as 0.258 nm, close to that for the OH group and H_2O molecule (0.252-0.277 nm), indicating the covalent bonding nature. Each α,ω -alkanedisulfonate ion is coordinated to two lanthanide ions from the neighboring two layers, bridging them into a hybrid 3D framework. In the gallery, relevant positions for O and S are split into two, and thus the linear alkanedisulfonate ions take two equivalent configurations. The alkyl chains are nearly parallel to the *ac* plane, but tilted toward the *bc* plane at an angle of $\sim 38.8^\circ$. Slot-like hydrophobic voids are noticed among these alkyl chains.

The organodisulfonate-series represent a new class of lanthanide-based inorganic-organic hybrid framework. Considering the flexibility of organic ligands, a large variety of hybrid frameworks based on the $\{[\text{RE}(\text{OH})_2(\text{H}_2\text{O})]^+\}_\infty$ layers can be expected. In view of the strong interaction between the organic pillars and RE ions, the

hybrid LREH series are anticipated to display new or tunable functionalities.

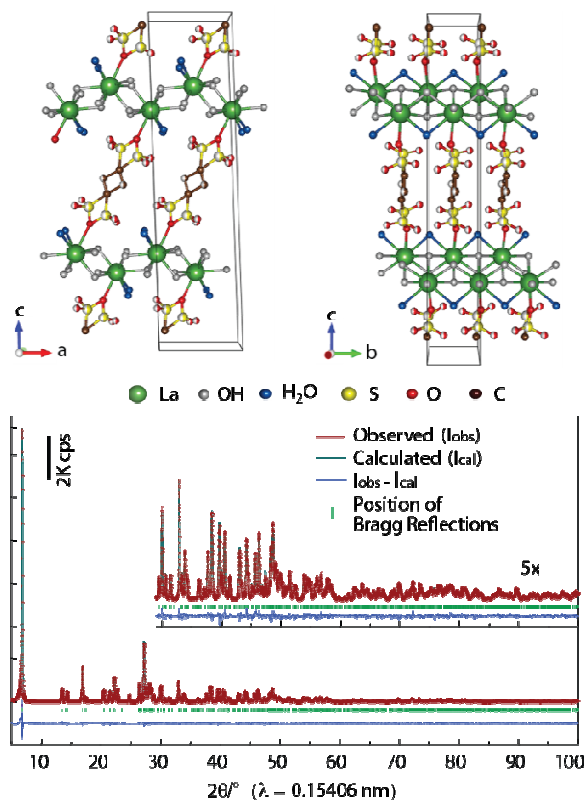


Fig. 8 Schematic illustration of crystal structure for $\text{La}_2(\text{OH})_4(\text{O}_3\text{S}(\text{CH}_2)_3\text{SO}_3) \cdot 2.2\text{H}_2\text{O}$. Adapted with permission from ref. 39. Copyright 2013 American Chemical Society.

4. Potential applications

4.1. Anion-exchange, swelling and exfoliation

The chloride- and nitrate-series of LREH compounds show facile anion-exchange behaviors at room temperature.³³⁻³⁶ Because anions in these LREH compounds are electrostatically accommodated between rare earth hydroxide layers, they can be readily exchanged with various species, being similar to that in LDH compounds. In contrast, for the sulfate- and organodisulfonate-series, the strong covalent interaction between the pillars and RE ions prevents these anions from being replaced at ambient conditions.

The anion-exchange reaction can be carried out by following simple procedures: immersing a sample in a solution containing excessive target anions, and the exchange

reaction proceeds to a completion generally within several hours at room temperature.^{33,35} XRD and FT-IR data clearly confirm the anion-exchangeability of these LREH compounds, as shown in Figure 9.³³ Similar to LDH compounds, such anion-exchange processes are believed to be driven in a toptactic manner, in which the host hydroxides layers are preserved without reconstruction.

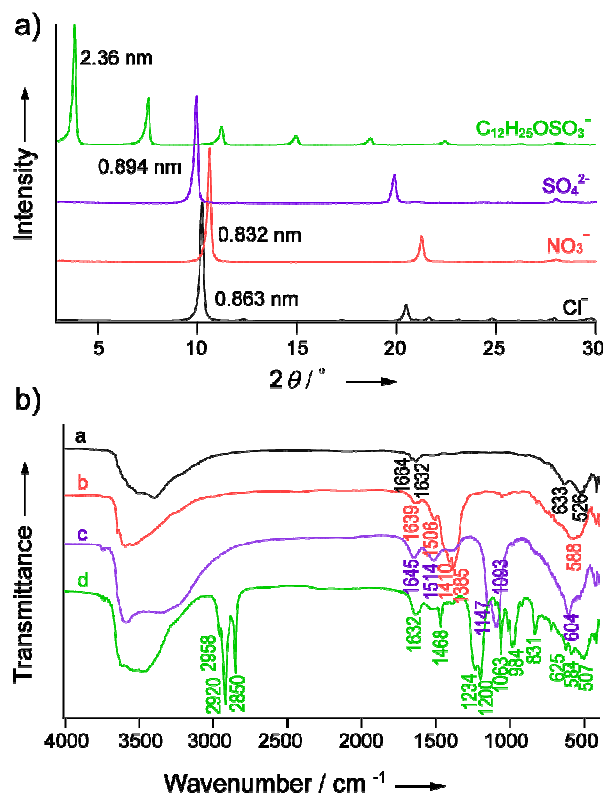


Fig. 9 XRD patterns (a) and FT-IR spectra (b) of as-obtained Cl^- form and its anion-exchanged samples. In figure (b), the curves from a to d represent the as-synthesized Cl^- form and the exchanged forms of NO_3^- , SO_4^{2-} and $\text{C}_{12}\text{H}_{25}\text{OSO}_3^-$ (DS^-), respectively. Adapted with permission from ref. 33. Copyright 2008 Wiley-VCH Verlag GmbH & Co. KGaA.

It should be noted that after conversion to the DS^- intercalated form, the LREH sample underwent swelling and exfoliation in formamide.⁴³ A stable dispersion could be obtained after vigorous agitation or ultrasonic treatment. The swelling and exfoliation process was confirmed by monitoring XRD pattern (Figure 10a). Atomic force microscopy (AFM) image detected extremely thin 2D crystallites with a very flat terrace

after drying a diluted sample on a substrate. The thickness of 1.6 nm provides clear evidence for the formation of unilamellar nanosheets (Figure 10 b). In-plane XRD data showed sharp diffraction peaks compatible with the 2D lattice from the original layered compounds. The obtained nanosheets can be taken as a new member of functional nanosheets. Similar to other oxide nanosheets as well as LDH nanosheets, they will be useful as a building block to fabricate nanostructured materials such as nanocomposites and nanofilms.^{45, 46}

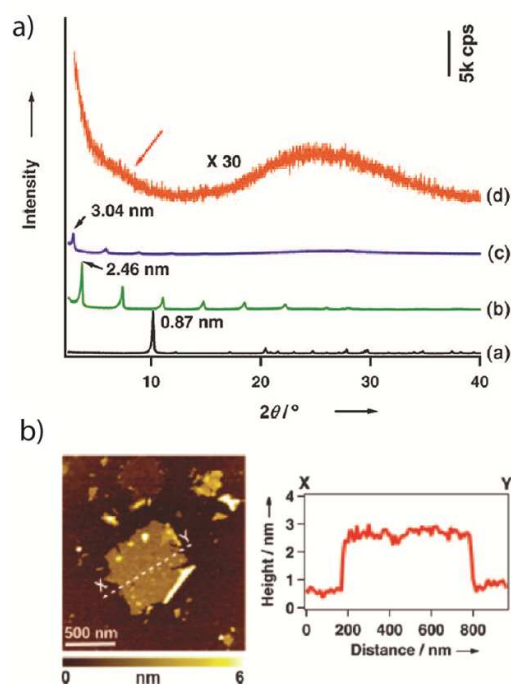


Fig. 10 a) XRD patterns of the Cl⁻ form (a), DS⁻ form (b), gels as the DS⁻ form mixed with formamide (c), and a colloidal aggregate obtained by centrifugation from the suspension (d). b) AFM image and the thickness profile of the nanosheet. Adapted with permission from ref. 43. Copyright 2010 Wiley-VCH Verlag GmbH & Co. KGaA.

4.2. Quasi-topotactic conversion into oxides

Dehydration and dehydroxylation of metal hydroxides are important for low-temperature production of metal oxide-based materials that are difficult to attain via conventional routes. Novel oxides, often metastable ones, are expected from the LREH compounds considering their unique combination of RE elements and guest anions.

Layered rare earth oxysulfates ($\text{Ln}_2\text{O}_2\text{SO}_4$) comprising $\{[\text{Ln}_2\text{O}_2]^{2+}\}_\infty$ layers are important for their high oxygen storage capability. Conventionally, polycrystalline samples were synthesized by heating sulfate salts of $\text{Ln}_2(\text{SO}_4)\cdot 8\text{H}_2\text{O}$ at temperature above 800°C or oxidation of Ln_2S_3 .⁴⁹ These synthetic routes are energy consuming, producing harmful waste gases of SO_3 and SO_2 . We have demonstrated that LREH compounds of $\text{Ln}_2(\text{OH})_4\text{SO}_4\cdot 2\text{H}_2\text{O}$ can transform into $\text{Ln}_2\text{O}_2\text{SO}_4$ samples via dehydration and dehydroxylation reactions, as shown in the example of Tb:³⁷



This synthetic route is environment-friendly, and proceeds at much lower temperature to produce the target phase. Unlike the heating of $\text{Ln}_2(\text{SO}_4)\cdot 8\text{H}_2\text{O}$ or oxidation of Ln_2S_3 which involves complicated reactions such as breaking of S-O bonding or oxidation of sulphide ions, this new route proceeds only via a dehydration/dehydroxylation step. FT-IR spectra revealed that both the LREH precursor and the target phase showed strong $\text{Tb}^{3+}\text{-SO}_4^{2-}$ covalent bonding, which should be the key reason for the low temperature transformation.

Thermal treatment of the organodisulfonate-series LREH compounds can result in hybrid oxides of $\text{Ln}_2\text{O}_2[\text{O}_3\text{S}(\text{CH}_2)_n\text{SO}_3]$.³⁹ For example, a sample formulated as $\text{La}_2\text{O}_2[\text{O}_3\text{S}(\text{CH}_2)_3\text{SO}_3]$ was formed after treating $\text{La}_2(\text{OH})_4(\text{O}_3\text{S}(\text{CH}_2)_3\text{SO}_3)\cdot 2.2\text{H}_2\text{O}$ at 275°C . The sample is crystallized in orthorhombic symmetry with cell parameters of $a = 0.8858(1)$, $b = 0.4250(1)$, $c = 2.4136(4)$ nm. Note that the parameters a and b are close to those in $\text{La}_2\text{O}_2\text{SO}_4$, a layered oxide containing infinite $\{[\text{La}_2\text{O}_2]^{2+}\}_\infty$ layers (cell parameters: $a = 1.4342(1)$, $b = 0.42827(3)$, $c = 0.83853(7)$ nm, and $\beta = 107.0(1)^\circ$).³⁹ Therefore, similar $\{[\text{La}_2\text{O}_2]^{2+}\}_\infty$ layers should be present in the $\text{La}_2\text{O}_2[\text{O}_3\text{S}(\text{CH}_2)_3\text{SO}_3]$ compound.⁵⁰ A structure model is proposed based on the lamellar structure of $\text{La}_2\text{O}_2\text{SO}_4$, as shown in Figure 11. As discussed below, such hybrid oxides act as unique hosts for accommodating luminescent RE centers for novel phosphors.

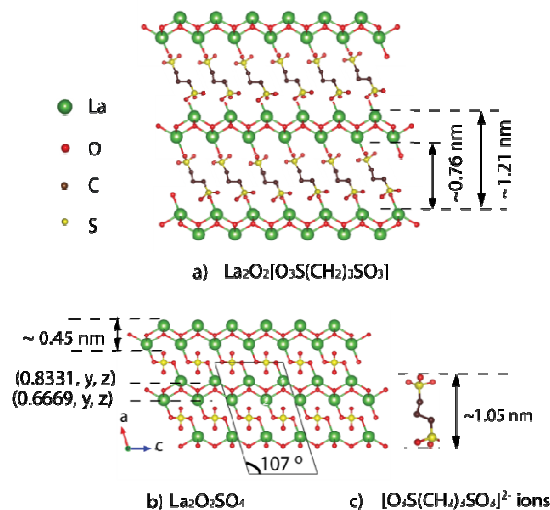


Fig. 11 Structure model of $\text{La}_2\text{O}_2[\text{O}_3\text{S}(\text{CH}_2)_3\text{SO}_3]$ derived by thermal treatment of $\text{La}_2(\text{OH})_4(\text{O}_3\text{S}(\text{CH}_2)_3\text{SO}_3) \cdot 2.2\text{H}_2\text{O}$. Adapted with permission from ref. 39. Copyright 2013 American Chemical Society.

4.3. Tunable phosphors

Thanks to the homogeneous alkalization reaction, various luminescent centers, typically Eu^{3+} and Tb^{3+} , can be incorporated in the hydroxide layers.^{37,39,40-42} Derived from the LREH compounds, high quality oxides with a tunable coordinative environment for these luminescent centers provide an opportunity for fabricating high performance phosphors.

Rectangle-shaped microcrystals of $(\text{Gd}_{0.95}\text{Eu}_{0.05})(\text{OH})_{2.5}\text{Cl}_{0.5} \cdot 0.9\text{H}_2\text{O}$ were synthesized through the homogeneous alkalization reaction. These crystals could be transferred onto a substrate after trapping them at a hexane/water interface.^{40,41} This unique process produced a monolayer film composed of densely packed platelet crystals having their face parallel to the substrate. Upon heating at 200-1000°C, the hydroxide film underwent quasi-topotactic transformation into a film of RE_2O_3 . The resulting oxide film was highly oriented along the (111) axis as a consequence of this unique process. The red emission was greatly enhanced to 527 times that of precursor powder samples thanks to this orientation.

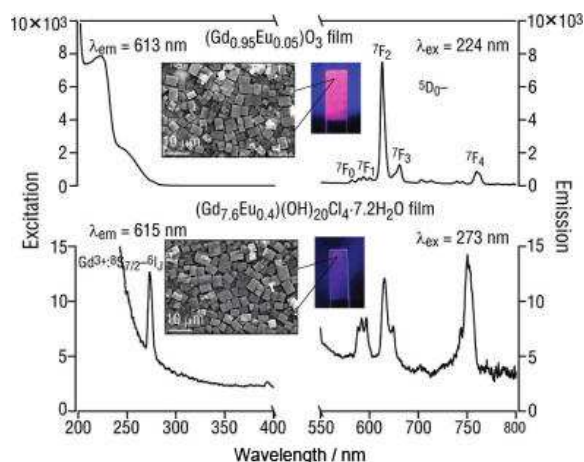


Fig. 12 Excitation and emission spectra for films of $(\text{Gd}_{0.95}\text{Eu}_{0.05})(\text{OH})_{2.5}\text{C}_{0.5}\cdot 0.9\text{H}_2\text{O}$ (bottom) and $(\text{Gd}_{0.95}\text{Eu}_{0.05})_2\text{O}_3$ (top). Insets are the corresponding SEM images and emission photographs under ultraviolet irradiation. Adapted with permission from ref. 41. Copyright 2009 Wiley-VCH Verlag GmbH & Co. KGaA.

Organic-inorganic hybrid phosphors were successfully obtained by incorporating Eu^{3+} or Tb^{3+} into the host of $\text{La}_2(\text{OH})_4(\text{O}_3\text{S}(\text{CH}_2)_3\text{SO}_3)\cdot 2.2\text{H}_2\text{O}$.³⁹ The typical red emission lines of Eu^{3+} and green emission lines of Tb^{3+} were observed. Because of the strong covalent interaction between the pillars and RE centers, the position and width of the red ${}^5\text{D}_0$ - ${}^7\text{F}_2$ line, which is very sensitive to the chemical environment of Eu^{3+} centers, can be tuned by changing the ligands. In addition, the red emission turned sharp and intense after the transformation into the hybrid oxide form. Moreover, Ce^{3+} ions, which tend to be easily oxidized into Ce^{4+} in air, could be stabilized in the hybrid host and provided an intense emission centered at 366 nm.

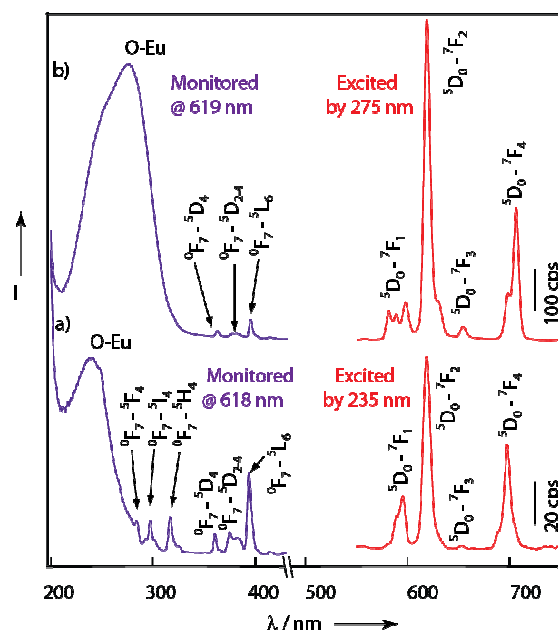


Fig. 13 Room-temperature excitation and emission spectra for samples with doping of 5% Eu^{3+} a) $\text{La}_2(\text{OH})_4[\text{O}_3\text{S}(\text{CH}_2)_3\text{SO}_3]\cdot 2\text{H}_2\text{O}$ and b) $\text{La}_2\text{O}_2[\text{O}_3\text{S}(\text{CH}_2)_3\text{SO}_3]$. Adapted with permission from ref. 39. Copyright 2013 American Chemical Society.

Conclusions and outlook

In summary, we applied the homogeneous alkalization route to synthesize LREH compounds. This method enabled the production of highly crystallized LREH compounds containing a range of anions, greatly expanding the varieties of the LREH family. The crystal structures of the LREH compounds have been solved and illustrated, correlating to their interesting behaviors such as anion-exchange, dehydration/rehydration, thermal phase evolution and so on. On the basis of crystal structure knowledge, LREH compounds have been explored as new functional materials as novel anion-exchangers, precursors to unusual oxides, and novel phosphors.

Our efforts in understanding the structure of LREH compounds have paved the avenue for their development as novel functional materials. This is just the start for this new research topic, and we believe that many opportunities can be explored from LREH

compounds, for example, coupling functional organic anions with the rare-earth hydroxide layers to build compounds having chiral structures. The magnetisms of LREH compounds may be an attractive subject in the future study, similar to those on transition metal hydroxides.^{51,52} As new layered hosts that combine the unique properties of RE elements and guest anions, the LREH compounds are expected to evoke interest in interdisciplinary fields, encompassing the environment, catalysis, and biology in the future.

Acknowledgements

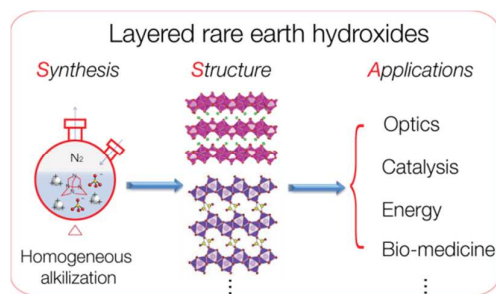
This work was supported by the World Premier International Center Initiative (WPI Initiative) on Materials Nanoarchitectonics (MANA), Ministry of Education, Culture, Sports, Science and Technology (MEXT) of Japan, and by the CREST program of the Japan Science and Technology Agency (JST).

Reference

1. J. C. G. Bunzli and C. Piguet, *Chem. Rev.*, 2002, **102**, 1897.
2. D. Parker, R. S. Dickins, H. Puschmann, C. Crossland and J. A. K. Howard, *Chem. Rev.*, 2002, **102**, 1977.
3. J. C. G. Bunzli, *Acc. Chem. Res.*, 2006, **39**, 53.
4. C. P. Montgomery, B. S. Murray, E. J. New, R. Pal and D. Parker, *Acc. Chem. Res.*, 2009, **42**, 925.
5. S. V. Eliseeva and J. C. G. Bunzli, *Chem. Soc. Rev.*, 2010, **39**, 189.
6. R. C. Ropp, *Luminescence and the Solid State*, 2nd edn, Elsevier Science, Amsterdam, 2004.
7. A. Kitai, *Luminescent Materials and Applications*, Wiley, New York, 2008.
8. L. Sorace, C. Benelli, D. Gatteschi, *Chem. Soc. Rev.*, 2011, **40**, 3092.
9. M. Shao, C. Li and J. Lin, *Chem. Soc. Rev.*, 2014, **43**, 1372.
10. L. D. Carlos, R. A. S. Ferreira, V. de Zea Bermudez and S. J. L. Ribeiro, *Adv. Mater.*, 2009, **21**, 509.
11. *Layered Double Hydroxides in Structure and Bonding*, ed. X. Duan and D. G. Evans, Series Editor D. M. P. Mingos, Springer-Verlag, Berlin, Heidelberg, 2006, vol. 119.

12. T. Stumpf, H. Curtius, C. Walther, K. Daedenne, K. Ufer and T. Fanghanel, *Environ. Sci. Technol.*, 2007, **41**, 3186.
13. Y. Chen, S. Zhou, F. Li, J. Wei, Y. Dai and Y. Chen, *J. Fluoresc.*, 2011, **21**, 1677.
14. P. Gunawan and R. Xu, *J. Phys. Chem. C*, 2009, **113**, 17206.
15. X. Gao, M. Hu, L. Lei, D. O'Hare, C. Markland, Y. Sun and S. Faulkner, *Chem. Commun.*, 2011, **47**, 2104.
16. Y. Zhao, J. G. Li, F. Fang, N. Chu, H. Ma and X. Yang, *Dalton Trans.*, 2012, **41**, 12175.
17. T. Posati, F. Bellezza, A. Cipiciani, F. Costantino, M. Nocchetti, L. Tarpani and L. Latterini, *Cryst. Growth Des.*, 2010, **10**, 2847.
18. R. F. Klevtsova and P. W. Klevtsova, *J. Struct. Chem.*, 1966, **7**, 524.
19. J. M. Haschke, and L. Eyring, *Inorg. Chem.*, 1971, **10**, 2267.
20. J. M. Haschke, *J. Solid State Chem.*, 1975, **12**, 115.
21. J. M. Haschke, *Inorg. Chem.*, 1974, **13**, 1812.
22. S. P. Newman and W. Jones, *J. Solid State Chem.*, 1999, **148**, 26.
23. F. Gándara, J. Perles, N. Snejko, M. Iglesias, B. Gómez-Lor, E. Gutiérrez-Puebla and M. Á. Monge, *Angew. Chem. Int. Ed.*, 2006, **45**, 7998.
24. L. J. McIntyre, L. K. Jackson and A. M. Fogg, *Chem. Mater.*, 2008, **20**, 335.
25. L. Poudret, T. J. Prior, L. J. McIntyre and A. M. Fogg, *Chem. Mater.*, 2008, **20**, 7447.
26. L. J. McIntyre, L. K. Jackson and A. M. Fogg, *J. Phys. Chem. Solids*, 2008, **69**, 1070.
27. S. A. Hindocha, L. J. McIntyre and A. M. Fogg, *J. Solid State Chem.*, 2009, **182**, 1070.
28. L. J. McIntyre, T. J. Prior and A. M. Fogg, *Chem. Mater.*, 2010, **21**, 2635.
29. K.-H. Lee and S.-H. Byeon, *Eur. J. Inorg. Chem.*, 2009, 929.
30. K.-H. Lee and S.-H. Byeon, *Eur. J. Inorg. Chem.*, 2009, 4727.
31. B.-I. Lee, K. S. Lee, J. H. Lee, I. S. Lee and S.-H. Byeon, *Dalton Trans.*, 2009, 2490.
32. Y.-S. Yoon, B.-I. Lee, K. S. Lee, G. H. Im, S.-H. Byeon, J. H. Lee and I. S. Lee, *Adv. Funct. Mater.*, 2009, **19**, 3375.
33. F. Geng, H. Xin, Y. Matsushita, R. Ma, M. Tanaka, F. Izumi, N. Iyi, and T. Sasaki,

- Chem.–Eur. J.*, 2008, **14**, 9255.
34. F. Geng, Y. Matsushita, R. Ma, H. Xin, M. Tanaka, F. Izumi, N. Iyi and T. Sasaki, *J. Am. Chem. Soc.*, 2008, **130**, 16344.
35. F. Geng, Y. Matsushita, R. Ma, H. Xin, M. Tanaka, F. Izumi, N. Iyi and T. Sasaki, *Inorg. Chem.*, 2009, **48**, 6724.
36. F. Geng, R. Ma and T. Sasaki, *Acc. Chem. Res.*, 2010, **43**, 1177.
37. J. Liang, R. Ma, F. Geng, Y. Ebina and T. Sasaki, *Chem. Mater.*, 2010, **22**, 6001.
38. F. Geng, R. Ma, Y. Matsushita, J. Liang, Y. Michiue and T. Sasaki, *Inorg. Chem.*, 2011, **50**, 6667.
39. J. Liang, R. Ma, Y. Ebina, F. Geng and T. Sasaki, *Inorg. Chem.*, 2013, **52**, 1755.
40. L. Hu, R. Ma, T. C. Ozawa, F. Geng, N. Iyi and T. Sasaki, *Chem. Commun.*, 2008, 4897.
41. L. Hu, R. Ma, T. C. Ozawa and T. Sasaki, *Angew. Chem. Int. Ed.*, 2009, **48**, 3846.
42. L. Hu, R. Ma, T. C. Ozawa and T. Sasaki, *Inorg. Chem.*, 2010, **49**, 2960.
43. L. Hu, R. Ma, T. C. Ozawa and T. Sasaki, *Chem.-Asian J.*, 2010, **5**, 248.
44. R. Ma, Z. Liu, L. Li, N. Iyi and T. Sasaki, *J. Mater. Chem.*, 2006, **16**, 3809.
45. R. Ma and T. Sasaki, *Adv. Mater.*, 2010, **22**, 5082.
46. T. Sasaki, *J. Ceram. Soc. Jpn.*, 2007, **115**, 9.
47. Z. Liu, R. Ma, M. Osada, K. Takada and T. Sasaki, *J. Am. Chem. Soc.*, 2005, **127**, 13869.
48. R. Ma, Z. Liu, K. Takada, N. Iyi, Y. Bando and T. Sasaki, *J. Am. Chem. Soc.*, 2007, **129**, 5257.
49. M. Machida, K. Kawamura, K. Ito and K. Ikeue, *Chem. Mater.*, 2005, **17**, 1487.
50. S. Zhukov, A. Yatsenko, V. Chernyshev, V. Trunov, E. Tserkovnaya, O. Anston, J. Höslä, P. Baulés and H. Schenk, *Mater. Res. Bull.*, 1997, **32**, 43.
51. É. Delahaye, S. Eyele-Mezui, M. Diop, C. Leucrey, P. Rabu and G. Rogez, *Dalton Trans.*, 2010, **39**, 10577.
52. C. Livage, N. Guilou, P. Rabu, P. Pattison, J. Marrot and G. Férey, *Chem. Commun.*, 2009, 4551.



Layered solid comprising cationic rare earth hydroxide layers has become a new source of multifunctionality.